Secure Systems Design and Technology Development. Veliko Tarnovo, Bulgaria
Proceedings of the International Scientific Conference, 2026. Volume II, 449-455

Development of a Method for Calibration of a Semiconductor Temperature Measurement Sensor

Tsanko Karadzhov
Department of Machine and Precision Engineering
Technical University of Gabrovo,
Center of competence "Smart mechatronic, eco-and energy-saving systems and technologies"
Gabrovo, Bulgaria
karadjov_st@abv.bg

Iliyan Gospodinov
Department of Machine and Precision Engineering
Technical University of Gabrovo,
Gabrovo, Bulgaria
gospodinov@tugab.bg

Dimitar Dichev
Department of Machine and Precision Engineering
Technical University of Gabrovo,
Center of competence "Smart mechatronic, eco-and energy-saving systems and technologies"
Gabrovo, Bulgaria
dichevd@abv.bg

Iliya Zhelezarov
Department of Machine and Precision Engineering
Technical University of Gabrovo
National Center of Excellence Mechatronics and Clean Technologies
Gabrovo, Bulgaria
izhel@tugab.bg

***Abstract*— Temperature is one of the most commonly measured quantities in science and industry. Temperature can have a significant impact on the course of various processes therefore, its accurate measurement and control is a task of particular importance for every process in everyday life, science, and industry. Precise temperature measurement is used in all fields - electronics, communications, mechanical engineering and medicine, and determines the quality of the manufactured product. In this study, an experimental calibration was performed on a semiconductor thermistor with a nominal resistance of 10 kΩ in the temperature range from 0°C to 90°C. Based on the experimental data obtained, the coefficients of the Steinhart–Hart equation were determined, which allow for a more precision determination of the temperature from the measured resistance of the sensor.**

Keywords*— *Semiconductor thermistor, Nominal resistance, Steinhart–Hart, Temperature measurement.

I. INTRODUCTION

Precise temperature measurement is one of the fundamental requirements in modern science, engineering, medicine, and industrial production. Temperature directly influences the physical, chemical, electrical, mechanical, and biological properties of materials and systems. Even small deviations in temperature may lead to significant changes in the behavior of technological processes, measurement accuracy, product quality, and operational safety. For this reason, the development and application of highly accurate temperature measurement methods have become an essential task in many scientific and industrial fields [6].

In scientific research, temperature measurements play a key role in experimental validation and data reliability. Many physical phenomena, including thermal expansion, electrical resistance variation, optical properties, and phase transitions, are strongly temperature-dependent. Consequently, insufficient temperature accuracy may introduce systematic errors and reduce the credibility of experimental results. High-precision temperature measurements are particularly important in metrology, nanotechnology, laser systems, and environmental monitoring, where external influences and thermal instability can significantly affect measurement uncertainty.

Precise temperature monitoring is equally important in medicine and healthcare. Medical diagnostics, laboratory analysis, sterilization procedures, and patient monitoring systems rely on accurate temperature determination. Small

Online ISSN 3044-7771
https://doi.org/10.68302/std2026.vol2.206

temperature variations can provide critical information about physiological conditions or the effectiveness of medical treatment. Similarly, in environmental sciences, precise temperature measurements are necessary for climate monitoring, atmospheric analysis, and ecological studies, where long-term accuracy and stability are essential for identifying trends and predicting environmental changes.

Therefore, the study and refinement of methods for precise temperature measurement are of great scientific and practical importance, and research in this field contributes to improving the reliability and accuracy of measurements.

II. Design of Hardware Platform for Temperature Measurement System Using an NTC Thermistor

The Hardware concept consists of the following modules:

ANALOG FRONT: This module contains two main blocks:

NTC DIVIDER: A voltadge divider composed of a precision reference resistor with a value of 10 kΩ and a 10 kΩ NTC thermistor. The midpoint of the divider sends a signal to the ADC module.

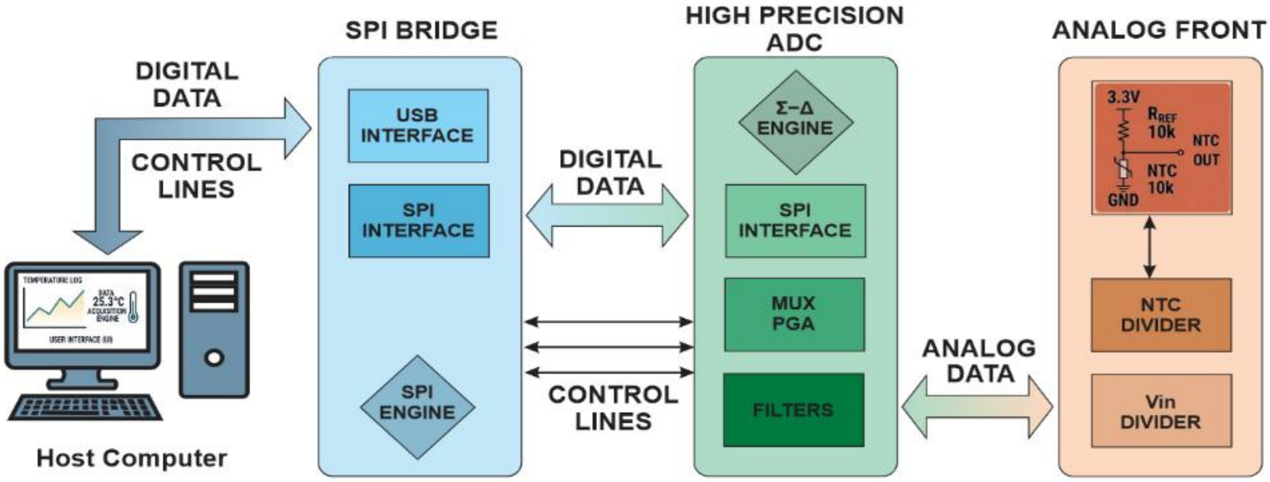

Fig. 1. Block diagram of the developed hardware platform for temperature measurement system.

Vref DIVIDER: A resistive divider consisting of 2 precision reference resistors that allow real-time measurement of the current power supply voltage. The midpoint of the divider sends a signal to the ADC module.

HIGH PRECISION ADC: Contains the following main blocks:

FILTERS: Built-in, software-controlled filters for noise suppression in various frequency ranges.

MUX, PGA: Multiplexer and amplifiers for reading data from multiple inputs simultaneously and amplifying the data when necessary.

Σ−Δ ENGINE: Ensures the conversion of analog signals from the sensors into a 24-bit digital signal with low noise.

SPI INTERFACE: A serial peripheral interface for communication with other devices.

SPI BRIDGE: Contains the following main blocks:

SPI INTERFACE: An interface that facilitates communication with peripheral devices communicating via a serial peripheral interface (SPI).

SPI BRIDGE: Contains the following main blocks:

SPI INTERFACE: An interface that enables communication with peripheral devices that communicate

via a Serial Peripheral Interface (SPI).The choice of this type of model is motivated by the need to ensure:

optimal recursive state estimation in the sense of minimum mean square error;

the possibility for explicit representation and adaptive handling of uncertainty sources through the covariance matrices;

agreement between the dynamic model and the measurement information under varying observation conditions.

The signal from the NTC sensor is fed into the NTC Divider via a voltage divider, the signal is sent to the ADC module. At the same time, a signal from the Vin Divider, containing the value of the supply voltage at the moment of measurement, is also sent to the ADC module. The two signals are read practically simultaneously in a single measurement cycle, filtered, digitized, and packaged into SPI packets, which are then transmitted via the SPI bus to the SPI Bridge module. The SPI Bridge module unpacks the SPI packet, repackages it into a USB packet, and transmits it to the USB interface. Via the USB interface, the host computer receives the data and transmits it for further processing to the DAQ software, which converts it into data suitable for direct reading by the operator.

The DAQ software provides the operator with data on the status of all modules during the measurement, the exact time of the measurement, the value of the supply voltage at the time of measurement (Vin), the voltage value at the midpoint of the divider in the NTC Divider (Vout), and the resistance value of the NTC sensor (Rntc) calculated using the formula

$$R_{NTC} = R_{ref} \frac{V_{out}}{V_{in} - V_{out}} \quad (1)$$

By including the measured input voltage Vin in the calculation for each measurement, the error caused by fluctuations in the supply voltage during the measurement process is effectively eliminated.

III. Software algorithm of the system

At the beginning, the program attempts to initialize the SPI module. Only a successful initialization leads to the next step, since without communication with the SPI module, subsequent communication with the ADC and reading data from the Analog Front module are not possible.

After successful initialization of the SPI module, an attempt is made to initialize the ADC module upon successful initialization, the operating mode and filters are configured, and the inputs for data reading are defined.

Data is read from the ADC, the read data is digitalized and formed into a packet that is sent to the SPI module for transmission. The SPI module converts the SPI packet into a USB packet and transfers it to the host computer via the USB interface [4].

The host computer receives the packet and passes it to the DAQ software, which calculates values for R and T and displays the data for Vin, Vout, R, and T to the operator.

The program terminates only if the operator press the button stop. Until this button is pressed, the cycle of reading, calculating, and visualizing the data runs automatically every 10 seconds.

The software module is developed in C# as a desktop application (Windows Forms) and is intended for periodic measurement and visualization of analog signals through an external measurement interface [7].

The application automatically initializes the connection, performs measurements at a defined interval, and calculates parameters such as voltage and resistance, while displaying and logging the results in real time.

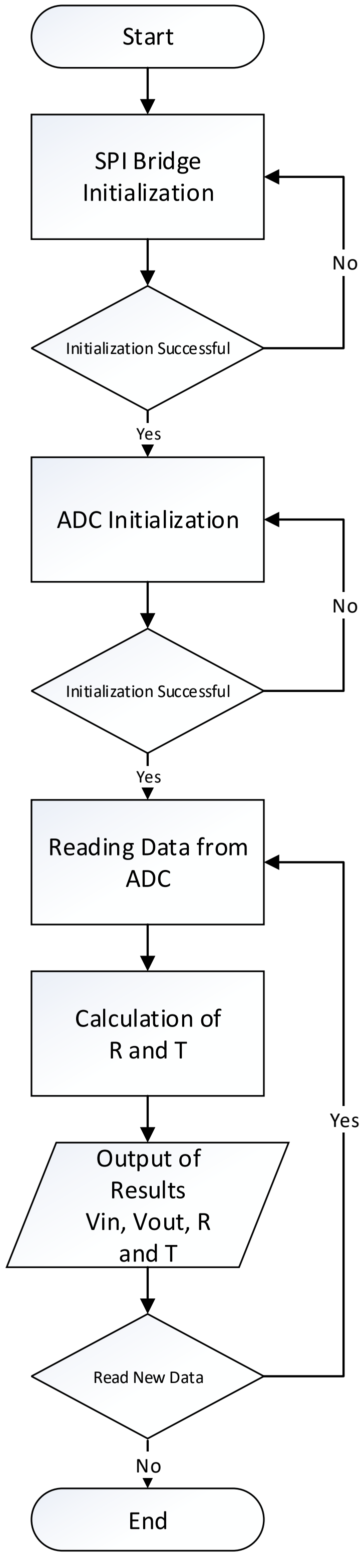

Fig. 2. Software algorithm of the system.

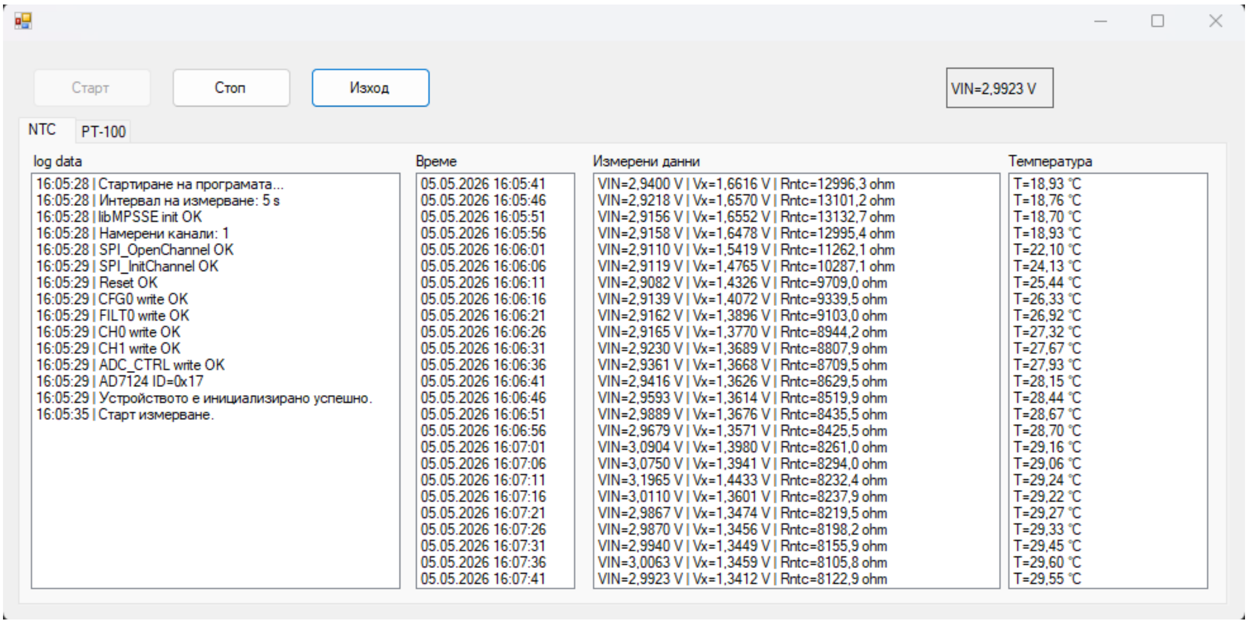

Fig. 3. User interface of the developed software module.

The software module allows for the initialization of the communication interface, the start and stop of the measurement process, as well as the real-time display of the measured parameters.

The interface displays and records data on the current status of the entire measurement circuit, the date and time of the measurement, the supply voltage at the time of measurement, the voltage across the thermistor divider, and the calculated thermistor resistance and temperature. System messages are displayed in separate information panels from the measurement data, allowing for quick differentiation between the measured values and fast, easy access to the information generated during system operation.

The developed software architecture ensures stable communication with the measurement hardware, periodic data collection from the sensors, automatic processing of the measured values, and continuous visualization of the calculated parameters.

IV. EXPERIMENTAL SETUP

Fig. 5 shows the experimental setup with which the measurements were made.

The temperature measurement and thermistor calibration system shown in the image represents a laboratory setup designed to create stable and controlled thermal conditions for accurate temperature measurements and calibration of thermistors. The system operates by heating a liquid medium inside a glass beaker while continuously mixing the liquid in order to maintain a uniform temperature distribution throughout the entire volume. At the base of the setup there is a constant-temperature magnetic stirrer that combines two important functions: controlled heating and magnetic stirring. The heating plate raises the temperature of the liquid bath to a desired value, while the magnetic stirring mechanism rotates a magnetic stir bar located inside the beaker. This continuous mixing process prevents the formation of local temperature gradients and ensures that all immersed sensors are exposed to the same thermal conditions.

Inside the beaker there is a distilled water for calibration procedures. The liquid serves as a thermal transfer environment with high heat capacity and good temperature uniformity. During operation, the heated liquid surrounds the temperature sensors and enables accurate transfer of thermal energy from the heater to the sensing elements. The magnetic stirring significantly improves the homogeneity of the temperature field, which is essential for precise calibration measurements because even small temperature differences within the liquid may introduce additional uncertainty in the obtained results.

Online ISSN 3044-7771
https://doi.org/10.68302/std2026.vol2.206

Fig. 4 Calibration measuring system

Two sensing elements are immersed in the liquid bath. One of them acts as a reference temperature sensor, usually a precision platinum resistance thermometer such as Pt100 with known metrological characteristics. This sensor provides the actual reference temperature of the liquid bath and serves as the standard against which the thermistor is calibrated. Alongside the reference sensor, the thermistor under investigation is also immersed in the liquid medium. The thermistor is positioned close to the reference sensor so that both devices experience nearly identical thermal conditions during the calibration process.

The entire sensing assembly is mounted using a laboratory support stand equipped with clamps and holders. This mechanical structure ensures stable positioning of the probes, constant immersion depth, and protection against movement caused by liquid stirring.

During operation, the temperature of the bath is gradually changed through a predefined range. At each temperature point, the value indicated by the reference thermometer is recorded together with the electrical resistance of the thermistor. These experimentally obtained temperature–resistance pairs are later used to determine the thermistor calibration characteristics and mathematical model. The Steinhart–Hart equation is used to describe the nonlinear relationship between thermistor resistance and temperature.

Using experimentally measured calibration points, the coefficients A, B, and C are calculated, allowing the thermistor to achieve significantly improved measurement accuracy over a wide temperature range.

V. Experimental Results

TABLE 1

R_t	T_1	T_2	T_3
Ω	°C	°C	°C
32470	0	0.11	-0.02
19790	10	10.12	9.96
11790	21	21.29	21.08
7945	30	30.33	30.07
5246	40	40.37	40.04
3560	50	50.30	49.88
2356	61	61.51	60.97
1716	70	70.60	69.96
1228	80	80.70	79.93
887	90	91.05	90.13

Table 1 shows the experimental measurement results. The experimental measurement results are shown in Table 1. T_1 denotes the temperature measured [9] by the reference sensor, T_2 denotes the temperature measured by the thermistor before calibration [10], and T_3 denotes the temperature measured by the thermistor after calibration.

The measurements obtained before calibration (T_2) show systematic deviations relative to the reference sensor (T_1). In nearly all measured points, the thermistor indicates temperatures higher than the reference values. The magnitude of the deviation increases with increasing temperature. At low temperatures, the error is relatively small, reaching only about +0.11 °C at 0 °C and +0.12 °C at 10 °C. However, as the temperature rises, the error becomes progressively larger. At 40 °C the deviation reaches approximately +0.37 °C, while at 70 °C and 80 °C the errors increase to approximately +0.60 °C and +0.70 °C, respectively. The largest deviation is observed at 90 °C, where the thermistor measurement before calibration differs from the reference value by approximately +1.05 °C. These results indicate that the uncalibrated thermistor exhibits nonlinear measurement errors that become increasingly pronounced at higher temperatures [13].

After calibration, the results represented by T_3 show a substantial improvement in accuracy. The measured temperatures become significantly closer to the reference sensor values across the entire measurement range. At 0 °C the deviation is reduced to approximately −0.02 °C, while at 10 °C the error becomes approximately −0.04 °C. In the middle part of the temperature range, the deviations remain very small, typically within ±0.1 °C. For example [11], at 30 °C the calibrated thermistor differs from the reference temperature by only +0.07 °C, and at 50 °C the deviation is approximately −0.12 °C. Even at higher temperatures, where the initial errors were most pronounced, the calibration significantly reduces the deviations [14]. At 80 °C the error decreases from approximately +0.70 °C before calibration to approximately −0.07 °C after calibration, while at 90 °C the deviation is reduced from +1.05 °C to approximately +0.13 °C.

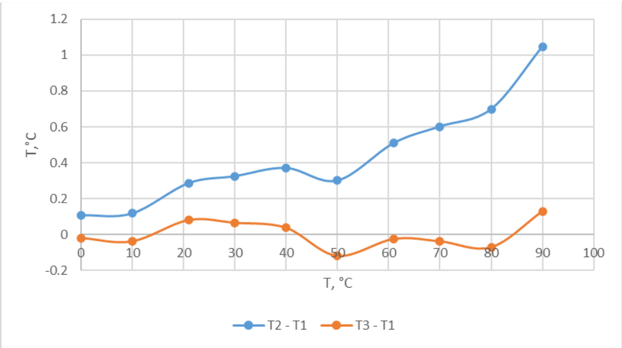

Fig. 5 Graphical representation of table 1

The obtained results demonstrate that the calibration process successfully compensates for the nonlinear characteristics and systematic measurement errors of the thermistor. The calibration procedure leads to a considerable reduction in measurement uncertainty and improves the agreement between the thermistor readings and the reference sensor values. Overall, the experimental data confirm that the applied calibration method provides a substantial enhancement in measurement accuracy over the entire investigated temperature range and makes the thermistor suitable for precision temperature measurement applications.

Fig. 6 shows the experimental characteristic of the tested NTC sensor [1].

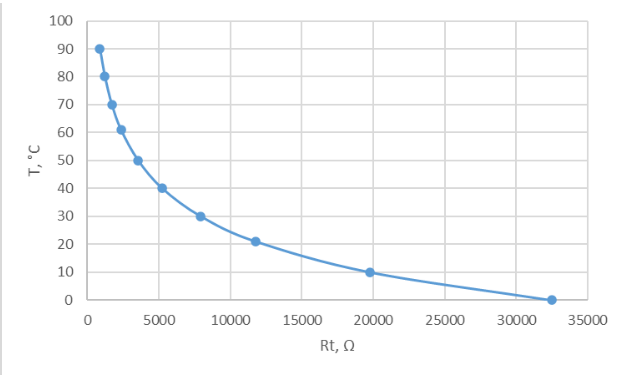

Fig. 6 Experimental Characterization of NTC Thermistor

VI. Methodology for Determining the Steinhart–Hart Coefficients

The temperature–resistance characteristic of the NTC thermistor is described by the Steinhart–Hart [8] equation:

$$\frac{1}{T} = A + B\ln(R_t) + C[\ln(R_t)]^3 \tag{2}$$

where T is the absolute temperature in Kelvin, R_t is the thermistor resistance in ohms, and A, B, and C are the unknown coefficients [12].

The first step is to convert all experimentally measured temperatures from degrees Celsius to Kelvin:

$$T_K = T_{°C} + 273.15 \tag{3}$$

Then, for each experimental resistance value R_t, the natural logarithm is calculated:

$$x = \ln(R_t) \tag{4}$$

After that, the third power of the logarithmic value is calculated:

$$x^3 = [\ln(R_t)]^3 \tag{5}$$

For every experimental point, one equation is obtained in the following form:

$$\frac{1}{T_i} = A + B\ln(R_i) + C[\ln(R_i)]^3 \tag{6}$$

For example, for the first experimental point:

$$T = 0°C$$

$$T_K = 273.15\ K$$

$$R_t = 32470\ \Omega$$

$$\ln(32470) = 10.3881$$

$$[\ln(32470)]^3 = 1120.89$$

$$\frac{1}{273.15} = 0.003661$$

Therefore, the first equation becomes:

$$0.003661 = A + 10.3881B + 1120.89C \tag{7}$$

The same calculation is performed for all experimental points. Since there are more than three experimental points, the system is overdetermined [15]. Therefore, the coefficients are not obtained from only three selected points, but from all measured points using the least-squares method.

The system can be written in matrix form [2] as:

$$Y = XK \tag{8}$$

where:

$$Y = \begin{bmatrix} 1/T_1 \\ 1/T_2 \\ 1/T_3 \\ \vdots \\ 1/T_n \end{bmatrix} \tag{9}$$

$$X = \begin{bmatrix} 1 & \ln(R_1) & [\ln(R_1)]^3 \\ 1 & \ln(R_2) & [\ln(R_2)]^3 \\ 1 & \ln(R_3) & [\ln(R_3)]^3 \\ \vdots & \vdots & \vdots \\ 1 & \ln(R_n) & [\ln(R_n)]^3 \end{bmatrix} \tag{10}$$

The least-squares solution is calculated by:

$$K = (K^T X)^{-1} X^T Y \tag{11}$$

After substituting the experimental data into the matrices and solving the system, the following coefficients are obtained:

$$A = 1.15970841 \times 10^{-3}$$

$$B = 2.30118380 \times 10^{-4}$$

$$C = 9.90697264 \times 10^{-8}$$

Therefore, the final Steinhart–Hart equation for the investigated NTC thermistor [5] is:

$$\frac{1}{T} = 1.15970841 \times 10^{-3} + 2.30118380 \times 10^{-4} \ln(R_t) + 9.90697264 \times 10^{-8}[\ln(R_t)]^3 \quad (12)$$

where T is in Kelvin and R_t is in ohms.

To calculate the temperature from a measured resistance value, the equation is rearranged as:

$$T_K = \frac{1}{A + B\ln(R_t) + C[\ln(R_t)]^3} \quad (13)$$

Finally, the temperature in degrees Celsius is obtained by:

$$T_{°C} = T_K - 273.15 \quad (14)$$

This procedure provides a mathematical model that represents the experimental temperature–resistance characteristic of the NTC thermistor with high accuracy [3].

VII. CONCLUSION

The experimental results demonstrate that the thermistor calibration procedure significantly improves the accuracy of temperature measurement over the entire investigated temperature range. Before calibration, the thermistor exhibited systematic measurement errors that increased with temperature, reaching deviations of more than 1 °C at higher temperatures. After calibration, the measured values became much closer to those obtained from the reference sensor, with most deviations reduced to within approximately ±0.1 °C. The calibration process successfully compensates for the nonlinear characteristics of the thermistor and substantially decreases measurement uncertainty. As a result, the calibrated thermistor provides considerably higher precision and reliability, making it suitable for accurate temperature measurement applications.

ACKNOWLEDGMENT

The authors acknowledge the support of the European Regional Development Fund, within the Operational Programme "Research, Innovation and Digitalization Programme for Intelligent Transformation 2021–2027", through Project No. BG16RFPR002-1.014-0006 for the experimental investigations and measurement equipment, and through Project No. BG16RFPR002-1.014-0005 for the theoretical development and analytical framework of the study.

REFERENCES

[1] J. S. Steinhart and S. R. Hart, "Calibration curves for thermistors," *Deep-Sea Research and Oceanographic Abstracts*, vol. 15, no. 4, pp. 497–503, 1968.

[2] C. Chen and Y. Chen, "Evaluation of resistance–temperature calibration equations for NTC thermistors," *Measurement*, vol. 42, no. 7, pp. 1103–1111, 2009.

[3] S. Rudtsch and C. von Rohden, "Calibration and self-validation of thermistors for high-precision temperature measurements," *Measurement*, vol. 76, pp. 1–6, 2015.

[4] M. Petkovšek, M. Jurčič, and D. Gleich, "Algorithm Execution Time and Accuracy of NTC Thermistor-Based Temperature Measurement Methods," *Mathematics*, vol. 9, no. 18, p. 2266, 2021.

[5] H. J. Hoge, "Useful procedure in least squares, and tests of some equations for thermistors," *Review of Scientific Instruments*, vol. 59, no. 6, pp. 975–979, Jun. 1988.

[6] A. Becker, "Properties and Uses of Thermistors—Thermally Sensitive Resistors," *Bell System Technical Journal*, vol. 26, no. 1, pp. 170–212, Apr. 1947.

[7] I. Balchev, A. Atanasov, A. Lengerov, and L. Lazov, "Investigation of the influence of the scanning speed and step in laser marking and engraving of aluminum," *Journal of Physics: Conference Series*, vol. 1859, no. 1, Art. no. 012002, Mar. 2021.

[8] Z. Liu, Y. Wang, and H. Zhang, "Design of a Negative Temperature Coefficient Thermistor Temperature Measurement System Based on the Steinhart–Hart Equation," *Sensors*, vol. 24, no. 9, pp. 1–18, 2024.

[9] G. Liu, L. Guo, C. Liu, and Q. Wu, "Evaluation of different calibration equations for NTC thermistor applied to high-precision temperature measurement," *Measurement*, vol. 120, pp. 21–27, May 2018, doi: https://doi.org/10.1016/j.measurement.2018.02.007.

[10] D. B. Deutz, S. van der Zwaag, and P. Groen, "Effect of particle contact on the electrical performance of NTC-epoxy composite thermistors," Materials Research Express, vol. 7, no. 1, Art. no. 015304, Jan. 2020.

[11] A. S. Bennett, "The calibration of thermistors over the temperature range 0–30 °C," *Deep-Sea Research and Oceanographic Abstracts*, vol. 19, no. 2, pp. 157–163, Feb. 1972, doi: https://doi.org/10.1016/0011-7471(72)90048-4

[12] D. Pulov, P. Tsvyatkov, "Passive Athermalization of Lenses for LWIR Spectral Range", in. Proceedings of the 16th International Scientific and Practical Conference Environment. Technology. Resources. Rezekne, Latvia, Volume 4, 329-335, 2025, DOI: https://doi.org/10.17770/etr2025vol4.8448.

[13] M. D. Alexander and K. T. B. MacQuarrie, "Toward a standard thermistor calibration method: Data correction spreadsheets," *Ground Water Monitoring & Remediation*, vol. 25, no. 4, pp. 75–81, Nov. 2005, doi: https://doi.org/10.1111/j.1745-6592.2005.00050.x.

[14] K. S. Gam, Y.-G. Kim, and I. Yang, "Calibration of Thermistors for Precision Temperature Measurements," *Journal of Sensor Science and Technology*, vol. 20, no. 5, pp. 329–335, 2011, doi: https://doi.org/10.5369/JSST.2011.20.5.329.

[15] S. K. Venkata, B. K. Roy, and N. Nair, "An adaptive calibration technique for thermistor with varying temperature coefficient and reference resistance," *F1000Research*, vol. 11, Art. no. 281, 2022, doi: https://doi.org/10.12688/f1000research.109226.1.